

Large-scale AlN nanowires synthesized by direct sublimation method

M. Lei^a, B. Song^b, X. Guo^b, Y.F. Guo^b, P.G. Li^a, W.H. Tang^{a,*}

^a Department of Physics, Center for Optoelectronics Materials and Devices, Zhejiang Sci-Tech University, Xiasha College Park, Hangzhou 310018, China

^b Beijing National Laboratory for Condensed Matter Physics, Institute of Physics, Chinese Academy of Sciences, Beijing 10080, China

Received 22 February 2008; received in revised form 10 June 2008; accepted 11 June 2008

Available online 21 July 2008

Abstract

Hexagonal aluminum nitride (AlN) nanowires were fabricated by direct sublimation method without a catalyst layer. The obtained nanowires have diameters of about 30–100 nm and length up to tens of micrometers. TEM observation indicates that these nanowires are single-crystalline and grow along [000 1] direction. It is thought that vapor–solid (VS) mechanism should be responsible for the growth of AlN nanowires. In addition, room temperature Raman scattering and photoluminescence spectra from AlN nanowires were studied. Photoluminescence spectrum of the AlN nanowires shows a wide emission band centered of 517 and 590 nm, which is related to N vacancies and the transition from the level of V_N^+ to ground state of the deep level of $[V_{Al}^{3-} + 3O_N^+]$ defects, respectively.

© 2008 Elsevier Ltd. All rights reserved.

Keywords: Nitrides; Nanowires; Sublimation method; Optical properties

1. Introduction

Research on the growth and properties of low-dimensional nanomaterials has attracted increasing attention due to their importance in both scientific research and technological applications.^{1–4} Aluminum nitride (AlN), one of wide band-gap semiconductors, is high attractive materials because of its high thermal stability, high dielectric breakdown strength, good mechanical strength, excellent chemical stability, nontoxicity, etc.^{5,6} Recently, low-dimensional AlN nanostructures such as nanowire, nanobelt and nanotube were found to possess promising applications in electronics and photonics devices.^{7–9} So far, various low-dimensional AlN materials such as nanowire, nanobelt, nanotube, nanoring, nanospring, etc. have been successfully synthesized by some methods including expanded VLS growth process,^{9–12} catalyst-assisted growth,^{13–16} direct nitridation,^{17–19} dc-arc plasma process²⁰ and carbothermal reduction.²¹ However, the direct sublimation method for synthesis of AlN nanowires has not been reported up to date. In this paper, by a direct sublimation process, large-scale AlN nanowires with hexagonal single-crystalline structure were synthesized at 1500 °C. The structural property, Raman scattering

and photoluminescence spectra of the AlN nanowires were characterized and investigated in detail.

2. Experimental

The synthesis of AlN nanowires was carried out in a horizontal tubular furnace with straight alumina tube, and AlN powders were used for synthesizing AlN nanowires under this study. The starting AlN powders were firstly ground for 30 h in a mechanical ball mill system. Then, 2 g ball-milled AlN powder (average size of 200 nm) was placed in an alumina boat. Another short alumina tube was eroded by NaOH at 500 °C for 5 min. First, the alumina boat was put into the eroded alumina tube. Then, both the alumina tube and the alumina boat were put in the center of the furnace. After flushed with Ar three times to remove the remaining air before each growth, the furnace temperature was first brought up to 800 °C under Ar flow rate of 80 sccm, and then Ar flow was placed by nitrogen flow at 30 sccm. The furnace temperature was continuously ramped up to 1500 °C and held at the temperature for 120 min. After the furnace temperature was cooled to the room temperature in the flow of nitrogen atmosphere, a large amount of gray white products were obtained from the inner surface of the eroded alumina tube.

Powder X-ray diffraction (XRD) data used for structural analysis was collected on PaNalytical X'Pert Pro MPD X-ray

* Corresponding author. Tel.: +86 571 86843468; fax: +86 571 86843222.
E-mail address: whtang@zstu.edu.cn (W.H. Tang).

diffractometer with Cu K α radiation. The morphology of the product was examined by field-emission scanning electron microscope (FEI XL30 S-FEG) equipped with energy-dispersive X-ray spectroscopy (EDS). The X-ray photoelectron spectra (XPS) were recorded on a VGESCALAB MKII X-ray Photoelectron Spectrometer, using non-monochromatized Mg K α X-ray as the excitation source. The chemical composition, TEM image, electron diffraction (ED) patterns and high-resolution lattice fringe (HRTEM) of samples were collected on the JEOL 2010 transmission electron microscope equipped with EDS. Raman measurement was performed on a multichannel modular tripe Raman system (JY-T64000) using a 514 laser as excitation source. Photoluminescence (PL) spectra of the nanowires were carried out at RT using the 325 nm line of a He–Cd laser with an output power of about 2 mW as the excitation source.

3. Results and discussion

Fig. 1a is the XRD pattern of the as-prepared sample. The diffraction peaks with miller indices marked above can be indexed to the hexagonal AlN, with lattice constants of $a=3.112 \text{ \AA}$, $c=4.982 \text{ \AA}$, agreeing well with the calculated diffraction pattern (ICDD-PDF No. 25-1133). No other impure

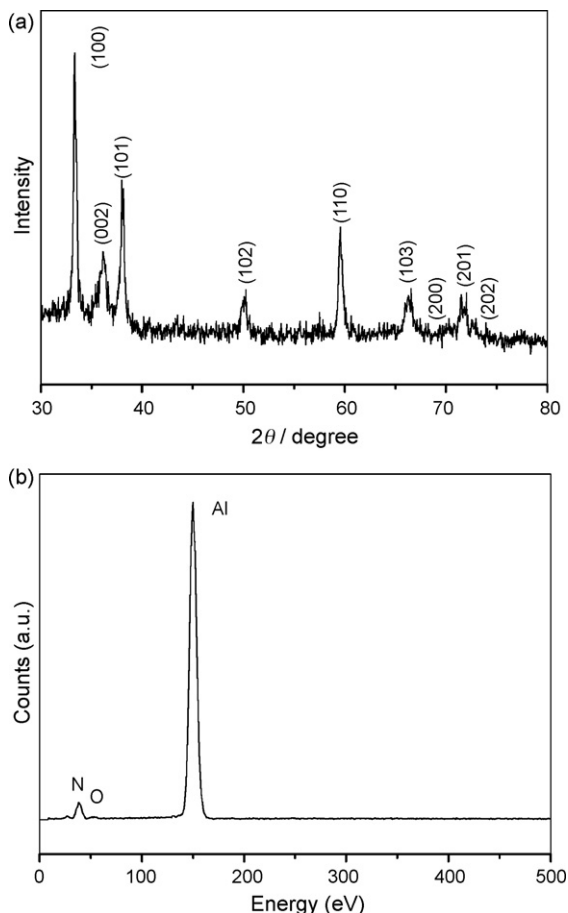


Fig. 1. (a) XRD pattern of the obtained AlN nanowires and (b) energy-dispersive X-ray analysis (EDX) of the AlN nanowires.

peaks are detected, indicating that the sample is predominantly hexagonal AlN. The composition of the as-prepared sample can be determined by the EDS analysis. The EDS (Fig. 1b) results indicate that the sample mainly consists of Al and N element. Trace amount of O element probably maybe comes from the O₂ and H₂O adsorbed on the sample surface and/or acts as impurity in interior structure of the sample. The average Al/N ratio is 1.08:1, indicating a little nitrogen-deficient condition or oxygen impurity of the sample. The composition of the sample can be also determined by XPS (Fig. 2). Fig. 2a shows a typical survey spectrum of the sample, indicating the presence of Al and N element. The appearance of O peaks is due to the O impurity of the sample. The binding energies, centered at 74.6 eV for Al 2p (Fig. 2b) and 397.8 eV for N 1s (Fig. 2c), are in good agreement with the values of the bulk and film AlN from the literature.²² Quantification of the Al 2p and N 1s peaks gives an average Al/N atomic ratio of 1.09:1, which is consistent with the EDS analysis, further confirms the nitrogen-deficient condition of the sample.

Typical SEM images of the sample are shown in Fig. 3. Clearly, Fig. 3a gives an overall view of the sample, revealing that there are large-scale AlN nanowires with high density. SEM image with higher magnification (Fig. 3b) reveals that the sample mainly consists of nanowires having diameters of around 30–100 nm and up to tens of microns in length with smooth surface and good toughness. Typical TEM images of the hexagonal AlN sample are shown in Fig. 4. Fig. 4a shows the low magnified TEM image of a single nanowire with diameter of approximately 30 nm. The EDS analysis of the nanowire (Fig. 4a) shows that the chemical composition mainly consists of Al and N element. O element is not detected maybe due to the limit of the instrumental resolution. The small amount of C and Cu elements come from the carbon-coated copper grid. The selected area electron diffraction (SAED) pattern taken from the nanowire (Fig. 4c) can be indexed based on the hexagonal AlN cell (ICDD-PDF No. 25-1133). The SAED pattern of the nanowire indicates the single-crystalline nature with $[0\ 1\ \bar{1}\ 0]$ zone axis and growth direction along $[0\ 0\ 0\ 1]$. HRTEM image of the nanowire shows spacings of 0.246 nm between two neighboring fringes, which corresponds to the d_{002} spacings of hexagonal AlN (Fig. 4d). In this direct sublimation route, catalyst is not used and the TEM analysis shows that no catalyst on the tip of the nanowires, indicating that the growth mechanism of the nanowires was not governed by vapor–liquid–solid (VLS) process. The trace of Na element on the surface can be detected due to the NaOH-etched process.²³ The trace of Na cannot play an important role in the Growth of AlN nanowires because we did not observed Na element in the AlN nanowires and the data about Na induced nanowire growth. Alkali halide instead of alkali can induce the growth of nanowires. The mechanism is alkali halide flux which can be applied to the growth of many kinds of nanowires such as metal oxides, metal carbides and other metal compounds.^{24–26} However, the experimental process and starting materials in the alkali halide flux is completely different from the process mentioned in this work. So, the growth of AlN nanowires is more likely to be controlled by the vapor–solid (VS) process. Since AlN is rather stable, AlN would not be decom-

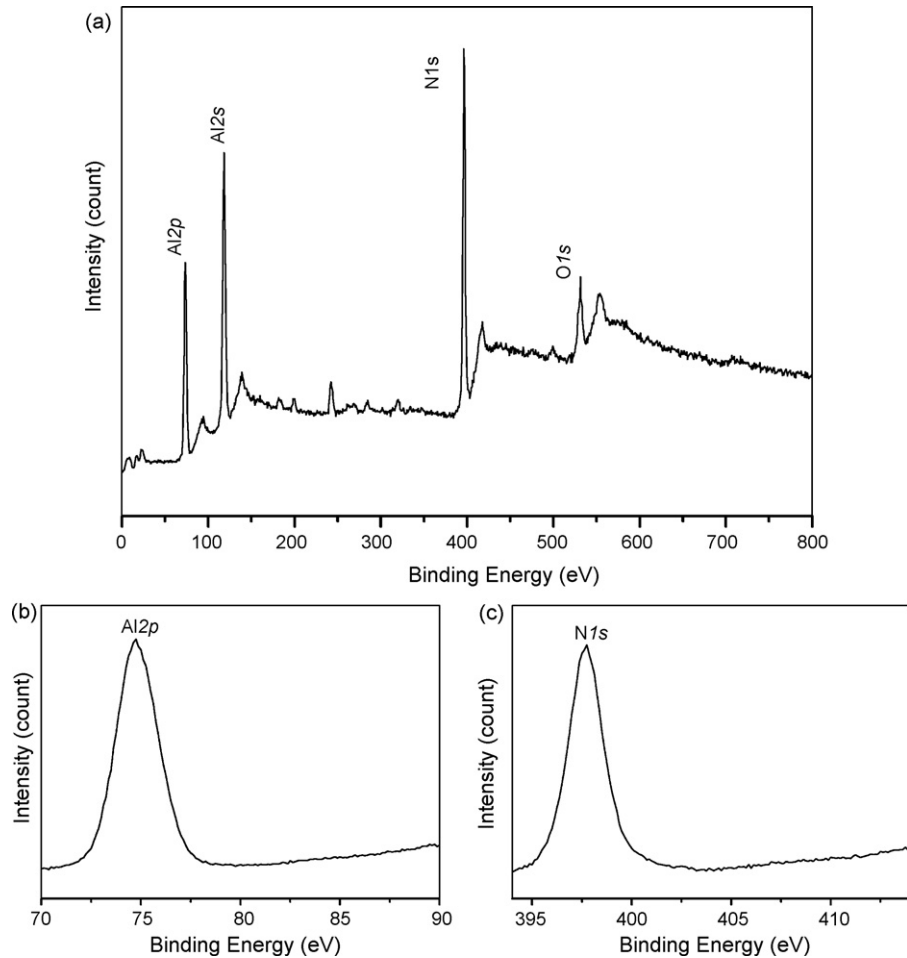


Fig. 2. XPS spectra of the obtained AlN nanowires: (a) N 1s region and (b) Al 2p region.

posed into Al vapor and N_2 at $1500^\circ C$. We deduce that AlN powders firstly sublime into gas-phase AlN at high temperatures. Subsequently, if the concentration of AlN is controlled to be low enough, in terms of the knowledge of crystallography, nanowires are expected to grow on the substrate at relative lower-temperature region. In this process, the surface defects of alumina tube play an important role in the formation of AlN nanowires. There are large amount of defects lying in the NaOH-etched alumina surface. These defects provide many nucleation sites for the growth of the AlN nanowires. If the surface of alumina surface is smooth, the experimental results show that only

polycrystalline AlN microparticles can be found. So, we deduce that the surface defects of alumina play an important role in the formation mechanism of AlN nanowires. However, the exact growth mechanism of AlN nanowires is not clear and needs to be further investigated.

The Raman spectrum of the hexagonal AlN nanowires was shown in Fig. 5. It is well known that the space group of hexagonal AlN is $C_4^{6v}(P6_3mc)$ with all atoms occupying the C_{3v} sites. Considering the Raman selection rules, six Raman-active modes may be present, i.e. $A_1(TO) + A_1(LO) + E_1(TO) + E_1(LO) + E_2(\text{high}) + E_2(\text{low})$ can

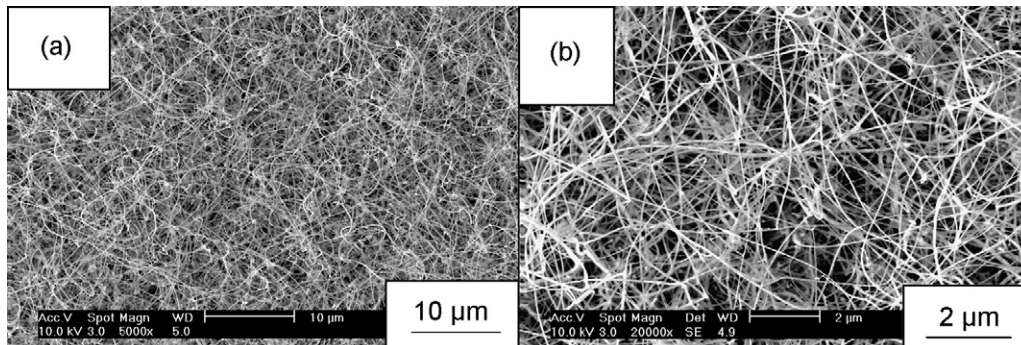


Fig. 3. (a) Low-magnification SEM image of the AlN nanowires and (b) high-magnification SEM image of the AlN nanowires.

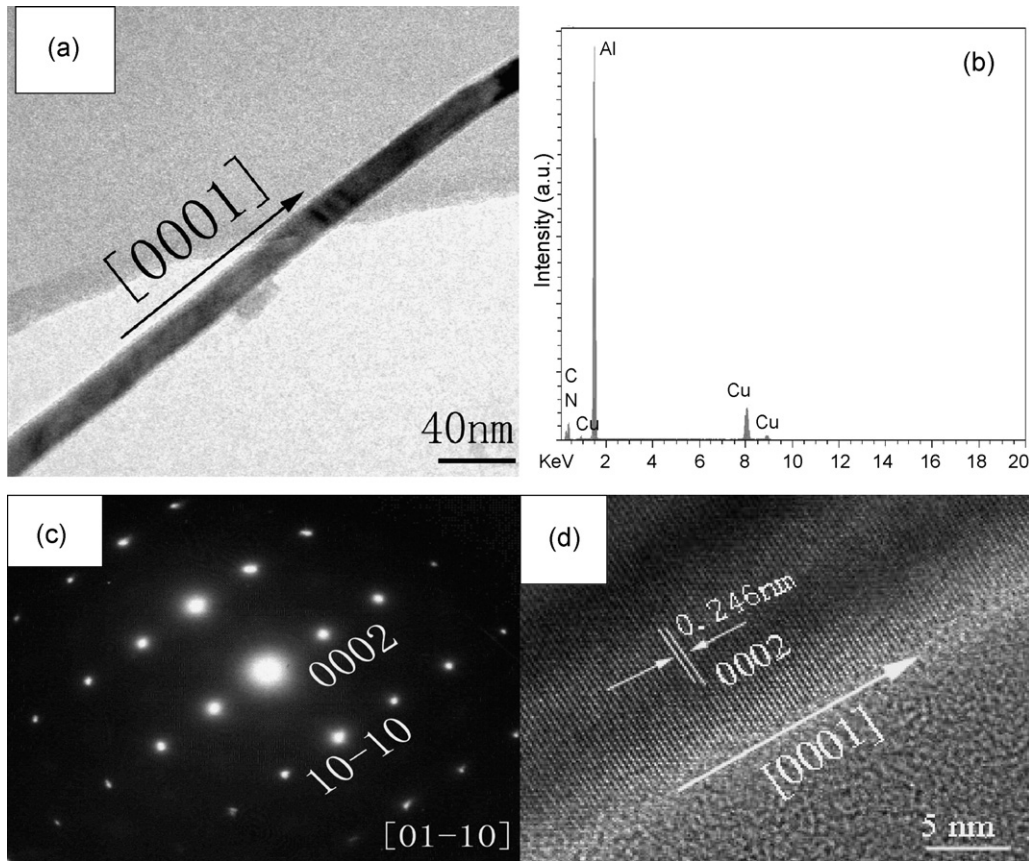


Fig. 4. (a) Typical TEM image of a single AlN nanowire; (b) EDS analysis of the single AlN nanowire; (c) SAED pattern of the AlN nanowire and (d) HRTEM images of the AlN nanowire.

be observed in the hexagonal AlN. In this study, five first-order Raman active phonons $A_1(\text{TO})$, $E_2(\text{high})$, $E_1(\text{TO})$, $A_1(\text{LO})$ and $E_1(\text{LO})$ at 607.8, 652.7, 665.2, 889.5 and 906.2 nm were observed, respectively. It is observed that these four modes are red-shift compared with the peaks from the AlN bulk and film data.²⁷ These red-shift phenomena can be also observed in other AlN nanostructures such as nanobelts, nanorings and nanoparticles.^{16–18,28} It is thought that the red-shift of these modes results from the size confinement effects and internal

stress.²⁹ $E_2(\text{low})$ mode is not observed here, which is permitted by $P6_3mc$ space group in the first-order Raman measurement at the zone center.

Fig. 6 shows the photoluminescence spectrum of the AlN nanowires excited at 325 nm. A wide emission band ranging from 1.55 eV (800 nm) to 3.59 eV (345 nm) centered at 2.4 eV (517 nm) and 2.1 eV (590 nm) is observed. The PL mechanism of wide emission band of AlN nanostructures had been extensively investigated. It is difficult to fabricate stoichiometric composition of AlN nanostructures. Up to now, pure band-edge emission

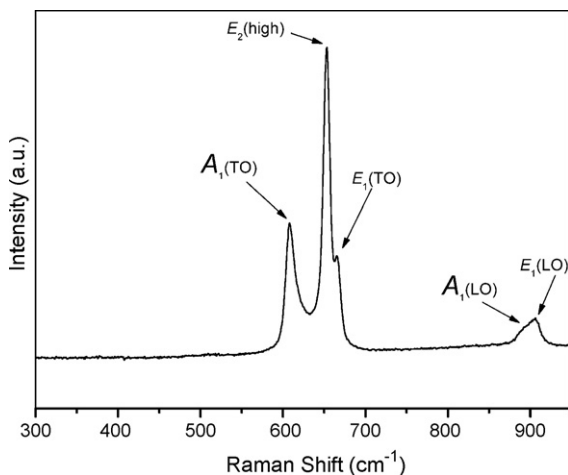


Fig. 5. Room-temperature Raman scattering spectrum of the AlN nanowires.

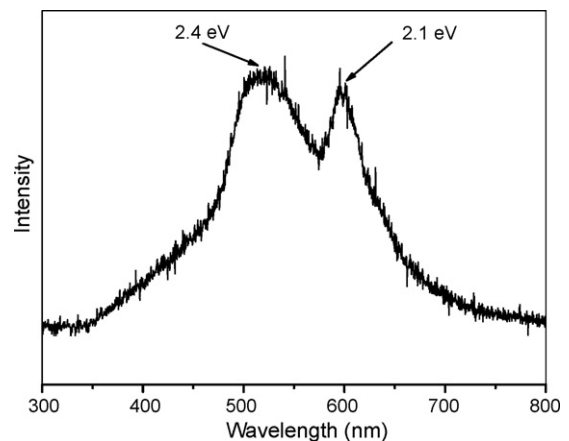


Fig. 6. Room-temperature PL spectrum of AlN nanowires.

(6.2 eV) of AlN nanostructured materials with stoichiometric composition has not been achieved and the mechanism of PL spectrum on the AlN nanostructures is rather complicated. The reported PL spectrum is completely different from each other. He et al.³⁰ reported the 2.39 eV band from AlN nanorods, which is similar to the 2.4 eV band emission in this work. It is thought N deficiency and the radiative recombination of a photon- (or electron-) generated hole with an electron occupying the N deficiency should be responsible for the emission band centered at 2.39 eV. Chen et al.³¹ observed three prominent luminescence bands at 2.1, 3.4 and the near band-edge 6.2 eV. They deduced that the low energy emission centered at 2.1 eV probably is the oxygen related luminescence centers. In addition, some literatures have reported other emission band centered at different energy such as 3.26, 2.75, 2.59, 2.02, 2.83 and 3 eV.^{32–38} It is generally believed that these low-energy emission is related to crystal defects or defect levels associated with nitrogen vacancy, oxygen-related centers (O_N^+), or aluminium interstitials that have formed during the growth, but without further giving exact explanations. The present results are closer to that of the literatures.^{30,31} It is thought that emission band at 2.4 eV is related to N vacancies and oxygen point defects should be responsible for the emission band at 2.1 eV. N vacancies as native defects confirmed by EDS and XPS analysis, are very common in the AlN nanomaterials. N vacancies and recombination of the generated holes with an electron occupying the N vacancies are main reason for the emission band centered at 2.4 eV. This phenomenon can be also observed in N-deficiency AlN thin films and nanoparticle structures.^{39,40} On the other hand, theoretically, the plane-wave pseudo-potential method was employed to calculate the oxygen point defects in AlN.⁴¹ The calculated results indicated that oxygen point defects in AlN could easily take the place of N to form deep level, and V_Al^{3-} and O_N^+ are the most favorable charged defects in AlN materials, and demonstrated the formation of $[\text{V}_\text{Al}^{3-} + 3\text{O}_\text{N}^+]$ defect complexes as deep level. In this work, oxygen impurity of AlN nanowires is confirmed by the EDS and XPS analysis, and the O in AlN can easily take the place of N form O_N^+ . We deduce that emission at 2.1 eV is attributed to the transition from the level of V_N^+ to ground state of the deep level of $[\text{V}_\text{Al}^{3-} + 3\text{O}_\text{N}^+]$ defect complexes, and it is in agreement with results reported by He et al.³¹

4. Conclusions

In conclusion, AlN nanowires with hexagonal crystal structure were successfully synthesized by direct sublimation method at 1500 °C. The experimental results indicate that these single-crystalline AlN nanowires have diameters of around 30–100 nm and up to tens of micron in length. These nanowires show the smooth surface and good toughness, and grow along [0001] direction. Photoluminescence spectrum of the AlN nanowires shows a wide emission band centered at 2.4 and 2.1 eV, respectively. It is found that emission band at 2.4 eV is related to N vacancies and emission band at 2.1 eV should be attributed to the transition from the level of V_N^+ to ground state of the deep level of $[\text{V}_\text{Al}^{3-} + 3\text{O}_\text{N}^+]$ defects.

Acknowledgements

This work was supported by the key project of the National Natural Science Foundation of China (60571029 and 50672088) and the Zhejiang Provincial Natural Science Foundation (Z605131).

References

- Cui, Y. and Lieber, C. M., Functional nanoscale electronic devices assembled using silicon nanowire building blocks. *Science*, 2001, **291**, 851–853.
- Cui, Y., Wei, Q. Q., Park, H. and Lieber, C. M., Nanowire nanosensors for highly sensitive and selective detection of biological and chemical species. *Science*, 2001, **293**, 1289–1292.
- Zhang, Y., Ichihashi, T., Landree, E., Nihey, F. and Iijima, S., Heterostructures of single-walled carbon nanotubes and carbide nanorods. *Science*, 1999, **285**, 1719–1722.
- Pan, Z. W., Dai, Z. R. and Wang, Z. L., Nanobelts of semiconducting oxides. *Science*, 2001, **291**, 1947–1949.
- Slack, G. A., Tanzilli, R. A., Pohl, R. O. and Vandersande, J. W., The intrinsic thermal conductivity of AlN. *J. Phys. Chem. Solids*, 1987, **48**, 641–647.
- Weimer, A. W., Cochran, G. A., Eisman, G. A., Henley, J. P., Hook, B. D., Mills, L. K. et al., Rapid process for manufacturing aluminum nitride powder. *J. Am. Ceram. Soc.*, 1994, **77**, 3–18.
- Duan, X. F., Huang, Y., Agrwal, R. and Lieber, C. M., Single-nanowire electrically driven lasers. *Nature*, 2003, **421**, 241–245.
- Huang, M. H., Mao, S., Feick, H., Yan, H. Q., Wu, Y. Y., Kind, H. et al., Room-temperature ultraviolet nanowire nanolasers. *Science*, 2001, **292**, 1897–1899.
- Wu, Q., Hu, Z., Zhang, X. Z., Lu, Y. N., Huo, K. F., Deng, S. F. et al., Extended vapor–liquid–solid growth and field emission properties of aluminium nitride nanowires. *J. Mater. Chem.*, 2003, **13**, 2024–2027.
- Wu, Q., Hu, Z., Wang, X. Z. and Chen, Y., Synthesis and optical characterization of aluminum nitride nanobelts. *J. Phys. Chem. B*, 2003, **107**, 9726–9729.
- Zhao, Q., Zhang, H. Z., Xu, X. Y., Wang, Z., Xu, J. and Yu, D. P., Optical properties of high ordered AlN nanowire arrays grown on sapphire substrate. *Appl. Phys. Lett.*, 2005, **86**, 193101–193103.
- He, J. H., Yang, R. S., Chueh, Y. L., Chou, L. J., Chen, L. J. and Wang, Z. L., Aligned AlN nanorods with multi-tipped surfaces-growth, field-emission and cathodoluminescence properties. *Adv. Mater.*, 2006, **18**, 650–654.
- Cimalla, V., Foerster, C., Cengher, D., Tonisch, K. and Ambacher, O., Growth of AlN nanowires by metal organic chemical vapour deposition. *Phys. Stat. Sol. (b)*, 2006, **243**, 1476–1480.
- Wang, H., Liu, G., Yang, W., Lin, L., Xie, Z., Fang, J. Y. et al., Bicrystal AlN zigzag nanowires. *J. Phys. Chem. C*, 2007, **111**, 17169–17172.
- Chen, Z., Cao, C. B. and Zhu, H. S., Controlled growth of aluminum nitride nanostructures: aligned tips, brushes, and complex structures. *J. Phys. Chem. C*, 2007, **111**, 1895–1899.
- Duan, J. H., Yang, S. G., Liu, H. W., Gong, J. F., Huang, H. B., Zhao, X. N. et al., AlN nanorings. *J. Cryst. Growth*, 2005, **283**, 291–296.
- Tian, Y. J., Jia, Y. P., Bao, Y. J. and Chen, Y. F., Macro-quantity synthesis of AlN nanowires via combined technique of arc plasma jet and thermal treatment. *Diamond Relat. Mater.*, 2007, **16**, 302–305.
- Xu, C. K., Xue, L., Yin, C. R. and Wang, G. H., Formation and photoluminescence properties of AlN nanowires. *Phys. Stat. Sol. (a)*, 2003, **243**, 329–335.
- Lei, M., Yang, H., Guo, Y. F., Song, B., Li, P. G. and Tang, W. H., Synthesis and optical property of high purity AlN nanowires. *Mater. Sci. Eng. B*, 2007, **143**, 85–89.
- Tondare, V. N., Balasubramanian, C., Shende, S. V., Joag, D. S., Godbole, V. P., Bhoraskar, S. V. et al., Field emission from open ended aluminum nitride nanotube. *Appl. Phys. Lett.*, 2002, **80**, 4813–4815.
- Zhang, Y. J., Liu, J., He, R. R., Zhang, Q., Zhang, X. Z. and Zhu, J., Synthesis of aluminum nitride nanowires from carbon nanotubes. *Chem. Mater.*, 2001, **13**, 3899–3905.

22. Wagner, C. D., Riggs, W. W., Davis, L. E., Moulder, J. F. and Muilenberg, G. E., Handbook of X-ray Photoelectron Spectroscopy. PerkinElmer Corporation, Physical Electronics Division, Eden Prairie, MN, 1979.
23. Cimalla, I., Will, F., Tonisch, K., Niebelschutz, M., Cimalla, V., Lebedev, V. et al., AlN/GaN bisensor-effect of device processing steps on the surface properties and biocompatibility. *Sensor. Actuat. B*, 2007, **123**, 740–748.
24. Wang, W. Z., Niu, J. Z. and Ao, L., Large-scale synthesis of single-crystal rutile SnO₂ nanowires by oxidizing SnO nanoparticles in flux. *J. Cryst. Growth*, 2008, **310**, 351–355.
25. Chen, Y. J., Li, J. B., Wei, Q. M. and Zhai, H. Z., Preparation and growth mechanism of TaCx whiskers. *J. Cryst. Growth*, 2001, **224**, 244–250.
26. Hayashi, S., Sugai, M., Nakagawa, Z., Takei, T., Kawasaki, K., Katsuyama, T. et al., Preparation of CaSiO₃ whiskers from alkali halide fluxes. *J. Eur. Ceram. Soc.*, 2000, **20**, 1099–1103.
27. Davydov, V. Y., Kitaev, Y. E., Goncharuk, I. N., Smirnov, A. N., Graul, J., Semchinova, O. et al., Phonon dispersion and Raman scattering in hexagonal GaN and AlN. *Phys. Rev. B*, 1998, **58**, 12899–12907.
28. Shi, S. C., Chen, C. F., Chattopadhyay, S., Lan, Z. H., Chen, K. H. and Chen, L. C., Growth of single-crystalline wurtzite aluminum nitride nanotips with a self-selective apex angle. *Adv. Funct. Mater.*, 2005, **15**, 781–786.
29. Shen, L. H., Li, X. F., Zhang, J., Ma, Y. M., Wang, Y., Peng, G. et al., Synthesis of single-crystalline wurtzite aluminum nitride nanowires by direct arc discharge. *Appl. Phys. A*, 2006, **84**, 73–75.
30. He, J. H., Yang, R., Chueh, Y. L., Chou, L. J., Chen, L. J. and Wang, Z. L., Aligned AlN nanorods with multi-tipped surfaces-growth, field-emission, and cathodoluminescence properties. *Adv. Mater.*, 2006, **18**, 650–654.
31. Shi, S. C., Chen, C. F., Chattopadhyay, S., Chen, K. H., Ke, B. W., Chen, L. C. et al., Luminescence properties of wurtzite AlN nanotips. *Appl. Phys. Lett.*, 2006, **89**, 163127–163129.
32. Zhao, Q., Zhang, H. Z., Xu, X. Y., Wang, Z., Xu, J., Yu, D. P. et al., Optical properties of highly ordered AlN nanowire arrays grown on sapphire substrate. *Appl. Phys. Lett.*, 2005, **86**, 193101–193103.
33. Wu, Q., Zhang, F., Wang, X. Z., Liu, C. and Hu, Z., Preparation and characterization of AlN-based hierarchical nanostructures with improved chemical stability. *J. Phys. Chem. C*, 2007, **111**, 12639–12642.
34. Chen, H. T., Wu, X. L., Xiong, X., Zhang, W. C., Wu, L. L., Zhu, J. et al., Formation mechanism and photoluminescence of AlN nanowhiskers. *J. Phys. D: Appl. Phys.*, 2008, **41**, 025101 (5pp).
35. Zhang, X. T., Liu, Z. and Hark, S. K., Synthesis and optical characterization of single-crystalline AlN nanosheets. *Solid State Commun.*, 2007, **143**, 317–320.
36. Yu, L. S., Hu, Z., Ma, Y. W., Huo, K. F., Chen, Y., Sang, H. et al., Evolution of aluminum nitride nanostructures from nanoflower to thin film on silicon substrate by direct nitridation of aluminum precursor. *Diamond Relat. Mater.*, 2007, **16**, 1636–1642.
37. Zheng, J., Song, X. B., Yu, B. and Li, X. G., Asymmetrical AlN nanopyramids induced by polar surface. *Appl. Phys. Lett.*, 2007, **90**, 193121–193123.
38. Tang, Y. B., Cong, H. T., Li, F. and Cheng, H. M., Synthesis and photoluminescent property of AlN nanobelt array. *Diamond Relat. Mater.*, 2007, **16**, 537–541.
39. Li, J., Nam, K. B., Nakarmi, M. L., Lin, J. Y. and Jiang, H. X., *Appl. Phys. Lett.*, 2001, **81**, 3365–3367.
40. Lan, Y. C., Chen, X. L., Cao, Y. G., Xu, Y. P., Xun, L. D., Xu, T. et al., Low-temperature synthesis and photoluminescence of AlN. *J. Cryst. Growth*, 1999, **207**, 247–250.
41. Mattila, T. and Nieminen, R. M., Ab initio study of oxygen point defects in GaAs, GaN and AlN. *Phys. Rev. B*, 1996, **54**, 16676–16682.